

Investigation of the Prototype Silylene Reaction, SiH₂ + H₂O (and D₂O): Time-Resolved Gas-Phase Kinetic Studies, Isotope Effects, RRKM Calculations, and Quantum Chemical Calculations of the Reaction Energy Surface

Rosa Becerra

Instituto de Química-Física “Rocasolano”, C.S.I.C., C/Serrano 119, 28006 Madrid, Spain

J. Pat Cannady

Dow Corning Corporation, P.O. Box 995, Mail 128, Midland, Michigan 48686-0995

Robin Walsh*

Department of Chemistry, University of Reading, Whiteknights, P.O. Box 224, Reading, RG6 6AD United Kingdom

Received: August 14, 2003; In Final Form: October 8, 2003

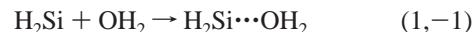
Time-resolved kinetic studies of the reaction of silylene, SiH₂, with H₂O and with D₂O have been carried out in the gas phase at 296 and at 339 K, using laser flash photolysis to generate and monitor SiH₂. The reaction was studied over the pressure range 10–200 Torr with SF₆ as bath gas. The second-order rate constants obtained were pressure dependent, indicating that the reaction is a third-body assisted association process. Rate constants at 339 K were about half those at 296 K. Isotope effects, k_H/k_D , were small averaging 1.076 ± 0.080 , suggesting no involvement of H- (or D-) atom transfer in the rate determining step. RRKM modeling was undertaken based on a transition state appropriate to formation of the expected zwitterionic donor–acceptor complex, H₂Si···OH₂. Because the reaction is close to the low pressure (third order) region, it is difficult to be definitive about the activated complex structure. Various structures were tried, both with and without the incorporation of rotational modes, leading to values for the high-pressure limiting (i.e., true second-order) rate constant in the range 9.5×10^{-11} to 5×10^{-10} cm³ molecule⁻¹ s⁻¹. The RRKM modeling and mechanistic interpretation is supported by ab initio quantum calculations carried out at the G2 and G3 levels. The results are compared and contrasted with the previous studies.

Introduction

Silylenes are of importance because they are implicated in the thermal and photochemical breakdown mechanisms of silicon hydrides and organosilanes, as well as being key intermediates in CVD. Time-resolved kinetic studies, carried out in recent years, have shown that the simplest silylene, SiH₂, reacts rapidly and efficiently with many chemical species.^{1,2} Examples of its reactions include Si–H bond insertions and C=C and C≡C π -bond additions.³ We have investigated the kinetics and mechanisms of a number of reactions of SiH₂^{4–18} including several of the prototype processes such as SiH₂ + SiH₄,⁷ SiH₂ + C₂H₄,⁶ and SiH₂ + C₂H₂.⁵ Reactions of silylenes with lone pair donors are another important reaction type,³ not least because in the case of O donors they lead to formation of the Si–O bond, the key linkage in silicone polymers. We have already studied the kinetics and potential energy surfaces of several reactions of SiH₂ with carbonyl containing compounds.^{12,14–16,18} In this paper, we turn our attention to SiH₂ + H₂O, which may reasonably be considered the prototype reaction of silylene with an n-type (lone pair) donor.

Alexander, King and Lawrance (AKL)¹⁹ have recently studied the kinetics of this reaction at 294 K and found it to be a pressure dependent, third-body assisted association process, consistent

with the reversible formation of a zwitterionic donor acceptor complex, viz.



By means of RRKM calculations, the second-order rate constants measured in the presence of argon (bath gas) were extrapolated to give an estimated rate constant at the high-pressure limit of 1.3×10^{-9} cm³ molecule⁻¹ s⁻¹. The RRKM model employed an E_0 value (approximately the binding energy of the complex) of 64.9 kJ mol⁻¹ compared with a quantum chemical (ab initio) calculated value of 52.3 kJ mol⁻¹.²⁰ Although there is a reasonable self-consistency in the conclusions of this work, the extrapolated second order rate constant is particularly high, as are others found by the King and Lawrance group for reactions of SiH₂ with other O donors.^{19,21} For reactions of SiH₂ with other species thought to be occurring at the collision rate, we have measured rate constants in the range $3-5 \times 10^{-10}$ cm³ molecule⁻¹ s⁻¹,^{6,7,12} but nothing higher than this.

We were thus stimulated to reinvestigate this system at room temperature, but also to investigate it at higher temperatures. To throw the maximum light on this system, we have investigated the reaction of SiH₂ with D₂O as well to obtain isotope effects. We additionally decided to reinvestigate the potential energy surface most recently studied by Heaven, Metha, and

* To whom correspondence should be addressed.

Buntine (HMB)²⁰ and earlier by others.^{22–24} A preliminary report of our work has appeared.²⁵

Experimental Section

Equipment, Chemicals, and Method. The apparatus and equipment for these studies have been described in detail previously.^{7,26} Only essential and brief details are therefore included here. SiH₂ was produced by the 193 nm flash photolysis of phenylsilane (PhSiH₃) using a Coherent Compex 100 exciplex laser. Photolysis pulses were fired into a variable temperature quartz reaction vessel with demountable windows, at right angles to its main axis. SiH₂ concentrations were monitored in real time by means of a Coherent 699-21 single-mode dye laser pumped by an Innova 90-5 argon ion laser and operating with Rhodamine 6G. The monitoring laser beam was multipassed between 32 and 48 times along the vessel axis, through the reaction zone, to give an effective path length of up to 1.8 m. A portion of the monitoring beam was split off before entering the vessel for reference purposes. The monitoring laser was tuned to 17259.50 cm⁻¹, corresponding to a known strong vibration–rotation transition^{26,27} in the SiH₂ A(¹B₁) ← X(¹A₁) absorption band. Light signals were measured by a dual photodiode/differential amplifier combination, and signal decays were stored in a transient recorder (Datalab DL910) interfaced to a BBC microcomputer. This was used to average the decays of between 5 and 30 photolysis laser shots (at a repetition rate of 0.5 or 1 Hz). The averaged decay traces were processed by fitting the data to an exponential form using a nonlinear least squares package. This analysis provided the values for first-order rate coefficients, k_{obs} , for removal of SiH₂ in the presence of known partial pressures of substrate gas.

Gas mixtures for photolysis were made up, containing between 1.3 and 3.1 mTorr of PhSiH₃, 0–12 Torr of H₂O (or D₂O), and inert diluent (SF₆) up to total pressures of between 10 and 200 Torr. Pressures were measured by capacitance manometers (MKS, Baratron).

All gases used in this work were thoroughly degassed prior to use. PhSiH₃ (99.9%) was obtained from Ventron-Alfa (Petrarch). H₂O (99.99%) was from local supply softened and demineralized, and D₂O (99.9%) was from Aldrich. Sulfur hexafluoride, SF₆, (no GC-detectable impurities) was from Cambrian Gases.

Ab Initio Calculations. The electronic structure calculations were performed with the Gaussian 98 software package.²⁸ All structures were determined by energy minimization at the MP2=Full/6-31G(d) level. Transition state structures were characterized as first-order saddle points by calculation of the Hessian matrix. Stable structures, corresponding to energy minima, were identified by possessing no negative eigenvalues of the Hessian, whereas transition states were identified by having one and only one negative eigenvalue. The standard Gaussian-3 (G3) compound method²⁹ was employed to determine final energies for all local minima. For transition states, four single-point energy determinations were carried out at the MP2 geometry, viz., QCISD(T)/6-31G(d), MP4/6-31+G(d), MP4/6-31G(2df,p), and optimized MP2=full/GTlarge, and the values were combined according to the G3 procedure.²⁹ The identities of the transition state structures were verified by calculation of intrinsic reaction coordinates³⁰ (IRC) at the MP2=Full/6-31G(d) or B3LYP/6-31G(d) levels. Reaction barriers were calculated as differences in G3 enthalpies at 298.15 K. These calculations were also carried out using the G2 method for comparison purposes.³¹

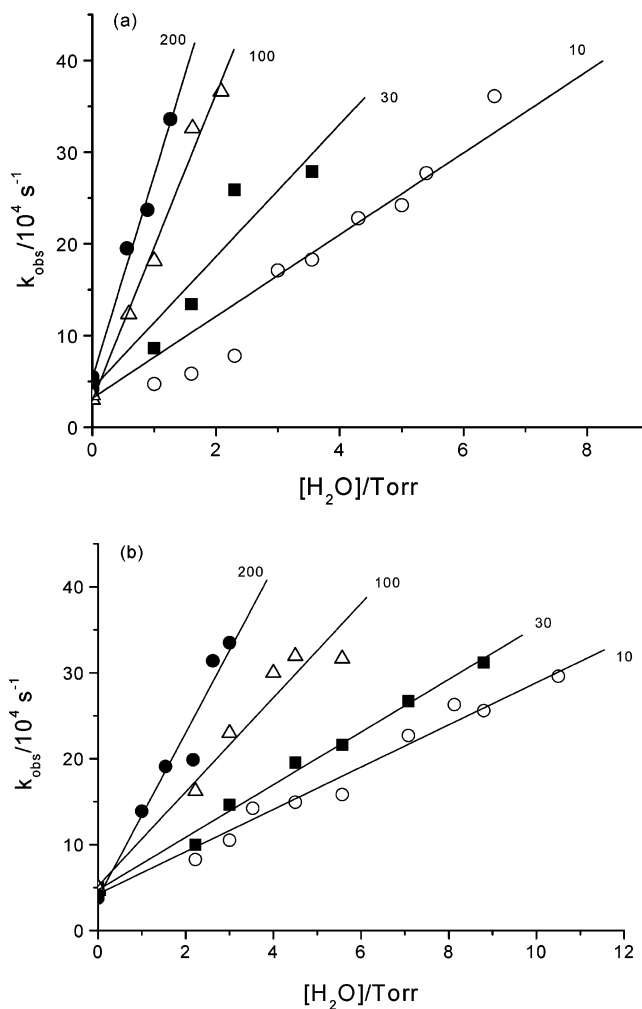


Figure 1. Second-order plots for the reaction of SiH₂ + H₂O at various total pressures. (○) 10 Torr, (■) 30 Torr, (△) 100 Torr, (●) 200 Torr. (a) $T = 296$ K. (b) $T = 339$ K.

Results

Kinetics. Preliminary experiments established that, for a given reaction mixture, decomposition decay constants, k_{obs} , were not dependent on the exciplex laser energy (45–70 mJ/pulse, routine variation) or number of photolysis shots (up to 30 shots). The constancy of k_{obs} (5 shot averages) showed no effective depletion of reactants. Higher pressures of precursor were required at the higher temperature because signal intensities decreased with increasing temperature. However, at each temperature, the precursor pressure was kept fixed. For each system (either SiH₂ + H₂O or SiH₂ + D₂O) at each temperature, a series of experiments was carried out at each of the four total pressures in the range 10–200 Torr. At each pressure (SF₆ diluent), four to eight runs (of 5–30 laser shots each) at different H₂O or D₂O pressures were carried out at each temperature. The results of these experiments are shown in Figures 1 and 2. These figures demonstrate, within reasonable experimental scatter, first the linear dependence of k_{obs} with substrate pressure expected for second order kinetics and second the strong overall pressure dependence of rates and therefore of the second-order rate constants. The second order rate constants derived from the gradients of these plots by least-squares fitting are shown in Table 1. The error limits are single standard deviations and are fairly small. As well as showing that the rate constants increase with increasing pressure, these results also show that they decrease with temperature (just as has been found in similar

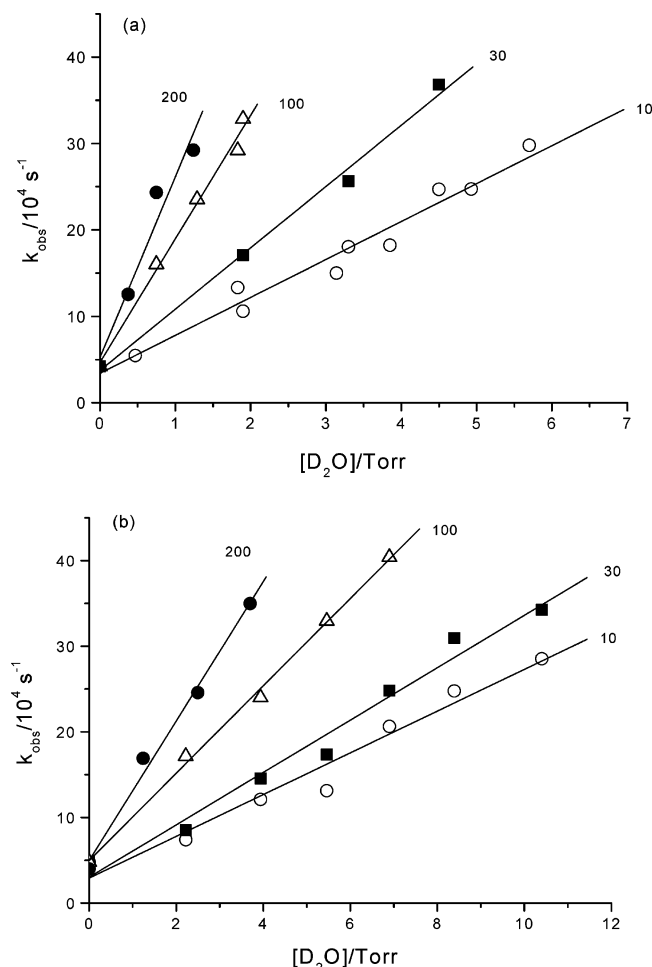


Figure 2. Second-order plots for the reaction of SiH₂ + D₂O at various total pressures. (○) 10 Torr, (■) 30 Torr, (△) 100 Torr, (●) 200 Torr. (a) *T* = 296 K. (b) *T* = 339 K.

TABLE 1: Experimental Second-Order Rate Constants for SiH₂ + H₂O and D₂O at 296 and 339 K and Various Pressures

<i>P</i> /Torr	<i>k</i> (H ₂ O) ^a	<i>k</i> (D ₂ O) ^a	<i>k_H</i> / <i>k_D</i>
<i>T</i> = 296K			
10	1.40 ± 0.09	1.32 ± 0.06	1.061 ± 0.083
30	2.35 ± 0.15	2.16 ± 0.07	1.088 ± 0.078
100	5.10 ± 0.19	4.44 ± 0.14	1.149 ± 0.056
200	6.76 ± 0.24	6.61 ± 0.56	1.023 ± 0.093
<i>T</i> = 339K			
10	0.863 ± 0.037	0.828 ± 0.063	1.042 ± 0.091
30	1.08 ± 0.03	1.048 ± 0.062	1.030 ± 0.067
100	1.92 ± 0.14	1.80 ± 0.04	1.066 ± 0.081
200	3.33 ± 0.24	2.90 ± 0.12	1.148 ± 0.095

^a Units: 10⁻¹² cm³ molecule⁻¹ s⁻¹.

SiH₂ association reactions^{5-7,9,12-15}). The rate constants for SiH₂ + D₂O are very similar in magnitude to those for SiH₂ + H₂O although there is a discernible isotope effect, favoring the latter reaction.

In this study, the rate measurements were limited to two temperatures, viz., 296 and 336 K. At higher temperatures, the quality of the reaction decay traces became poorer (signal decays not exponential with slow return to baseline). This is probably due to the onset of reversibility, as observed by AKL in the SiH₂ + MeOH¹⁹ and SiH₂ + Me₂O²¹ reaction systems. The pressure range was dictated by practical considerations. The lowest pressure of 10 Torr was governed by the need to have sufficient substrate pressure to observe reaction. The highest

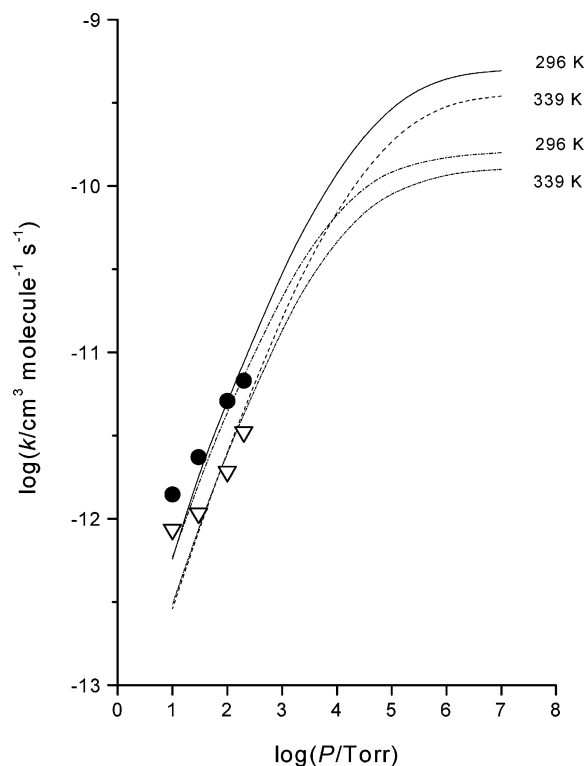
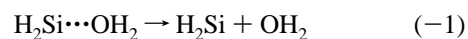


Figure 3. Pressure dependence of the second-order rate constants for SiH₂ + H₂O at 296 K (■) and 339 K (▽). Lines are RRKM fits corresponding to different transition states: TSA (—, ---), TSb (— · —, ···). See text for details.

pressure was 200 Torr. At higher pressure, the SiH₂ signals were partially quenched, and reliable decays were impossible to obtain. The temperature range of 40 K is insufficient to obtain reliable Arrhenius parameters, but from the average decrease in rate constant between 296 and 339 K, an activation energy of ca -14 (±5) kJ mol⁻¹ is calculated.

The overall pressure dependences for the SiH₂ + H₂O system are plotted in Figures 3–5 where they are compared with the results of RRKM (Rice, Ramsperger, Kassel, Marcus) calculations for various transition state models. The pressure dependences for SiH₂ + D₂O were very similar and are not shown. The pressure and temperature effects are consistent with those of a third body assisted association process although not as extensive as those obtained in other such reaction systems of silylene.^{5-7,9,12,13,15} The RRKM calculations³² are described in the next section.

RRKM Calculations. The pressure dependence of an association reaction corresponds exactly to that of the reverse unimolecular dissociation process providing there are no other perturbing reaction channels. The ab initio calculations do not suggest any such channel, and so we have carried out RRKM calculations on the unimolecular dissociation of the zwitterion, donor–acceptor complex, H₂Si···OH₂, viz.



Because the H₂Si···OH₂ molecule has not been isolated, let alone studied, we are forced to make estimates of the necessary parameters for these calculations. This has been done as follows. First the ab initio calculations were used to calculate the statistical mechanical standard entropies, *S*[°], of the species involved in the equilibrium reaction (1, -1). The values obtained, *S*[°](SiH₂) = 207 J K⁻¹ mol⁻¹ and *S*[°](H₂O) = 188 J K⁻¹ mol⁻¹, are in good agreement with literature.³³ The value for *S*[°](H₂-

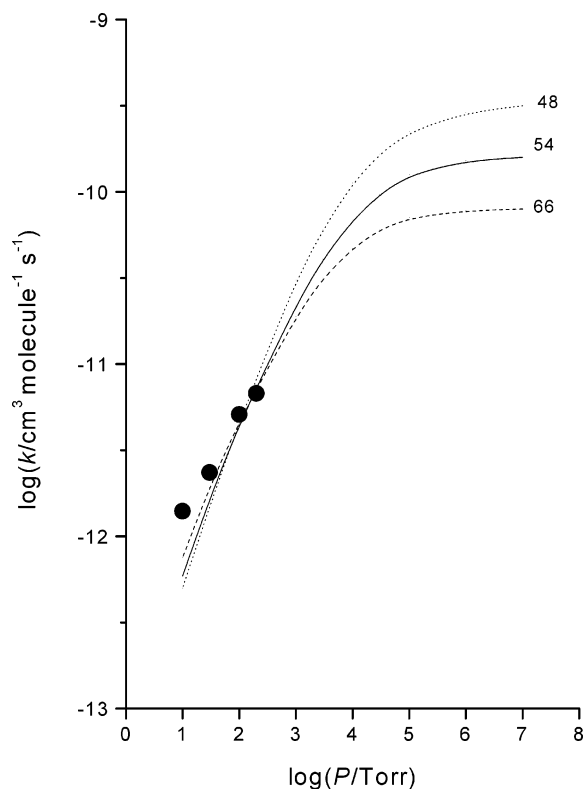


Figure 4. Comparison of RRKM calculated curves for three different critical energies at 296 K (data points, ●). For each curve, the value of $E_0/kJ\ mol^{-1}$ is given.

$Si\cdots OH_2$) was $270\ J\ K^{-1}\ mol^{-1}$, leading to a $\Delta S^\circ(-1,1)$ value of $+125\ J\ K^{-1}\ mol^{-1}$. Using the relationship, $\ln(A_{-1}/A_1) = \Delta S^\circ(-1,1)/R$ where A_{-1} and A_1 are the respective dissociation and association A factors (and with modification of $\Delta S^\circ(-1,1)$ to molecular concentration units at 298 K) leads to $A_{-1}/A_1 = 3.10 \times 10^{25}\ molecule\ cm^{-3}$. This value was used to constrain the magnitude of the dissociation A factor, A_{-1} , as follows. Typical values of A factors for SiH_2 association reactions which occur with high collisional efficiency are ca. $1.0 \times 10^{-10}\ cm^3\ molecule^{-1}\ s^{-1}$.^{1,2} Thus, to cover the possibilities of both looser and tighter than normal A factors, values of 3.0×10^{-10} and $3.0 \times 10^{-11}\ cm^3\ molecule^{-1}\ s^{-1}$ were chosen for A_1 . These values correspond to values of A_{-1} of ca. $1.0 \times 10^{16}\ s^{-1}$ and $1.0 \times 10^{15}\ s^{-1}$ respectively, at 296 K. These values are both lower than the ca. $4 \times 10^{16}\ s^{-1}$ used by AKL.¹⁹ A slight lowering of A by $10^{-0.06}$ ($=0.87$) was imposed on the transition states at 339 K concordant with our modeling findings in

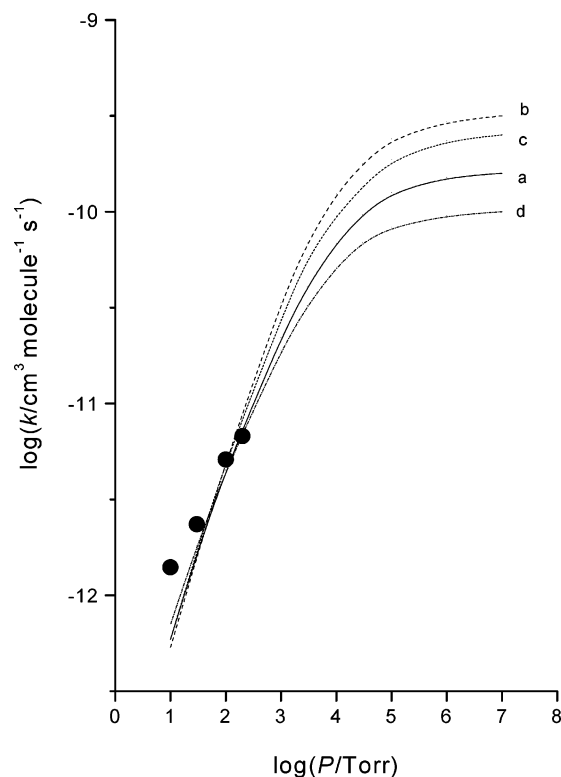


Figure 5. Comparison of RRKM calculated curves for four different TS models at 296 K (data points, ●). All models correspond to $\log(A/s^{-1}) = 15.0$: a. TSb, vibs only; b. TSb with internal rotation replacing torsion; c. TSb and reactant molecule with internal rotation replacing torsion; d. TSb with active external rotation.

previous systems.^{6,7,9,12,15} The parameters used in the initial RRKM calculations are shown in Table 2. This lists the molecular vibrational wavenumbers for $H_2Si\cdots OH_2$ obtained from the ab initio calculations corrected by the 0.893 factor appropriate to this level. The values for the two transition states TSa and TSb were obtained by adjustment of the wavenumbers for the five modes associated with OH_2 and SiH_2 group rocking and wagging and the $Si\cdots O$ torsion. The $Si-O$ stretching mode was taken as the reaction coordinate. Although these wavenumber adjustments are somewhat arbitrary, it is well-known that the outcome of the calculations is not sensitive to precise values as long as the entropy of activation (i.e., the magnitude of the A factor) is correctly matched. It is worth pointing out that these TS assignments are essentially vibrational, in that all modes are treated as harmonic oscillators. Exploration of other possibilities is considered later. In modeling the collisional

TABLE 2: Molecular and Transition State Parameters for RRKM Calculations for Decomposition of the $H_2Si\cdots OH_2$ Adduct

parameter	molecule	TS complex			
		TSa (296 K)	TSa (339 K)	TSb (296 K)	TSb (339 K)
O-H str(2)	3715	3715	3715	3715	3715
	3613	3613	3613	3613	3613
Si-H str(2)	1965	1965	1965	1965	1965
	1918	1918	1918	1918	1918
OH_2 bend	1611	1611	1611	1611	1611
SiH_2 bend	997	997	997	997	997
Si-O str	776	rxn coord	rxn coord	rxn coord	rxn coord
OH_2 wag	509	102	120	180	190
OH_2 rock	408	100	105	150	150
SiH_2 wag	651	130	130	200	235
SiH_2 rock	257	70	75	100	110
$Si\cdots O$ torsion	154	40	45	75	80
A/s^{-1}		1.0×10^{16}	8.8×10^{15}	1.0×10^{15}	8.7×10^{14}
$E_0/kJ\ mol^{-1}$		65	65	54	54
$Z/10^{-10}\ cm^3\ molec^{-1}\ s^{-1}$		4.38	4.46	4.38	4.46

deactivation process, we have used a weak collisional (step-ladder) model,³² because there is considerable evidence against the strong collision assumption.³⁴ The average energy removal parameter, $\langle\Delta E\rangle_{\text{down}}$, which determines the collisional efficiency was taken as 12.0 kJ mol⁻¹ (1000 cm⁻¹), similar to that used in previous systems (with SF₆ bath gas^{6,15}). The calculations were fairly insensitive to this value, because effectively, at lowish temperatures, this corresponded to close to strong collisions. They are however significantly stronger than those for Ar bath gas, viz., 3.8 kJ mol⁻¹ (320 cm⁻¹), used in the calculations (and experiments) of AKL.¹⁹

The critical energy, E_0 , was treated as a semi-adjustable parameter, because there is insufficient information to use it to fit the data unambiguously. Thus, the range of values considered was 48–66 kJ mol⁻¹ (11.6–15.8 kcal mol⁻¹) centered around the ab initio value calculated both by us and in previous work.^{19,20} Figure 3 shows the results of two sets of calculations at each temperature of study: the first set with the higher A factors (TSa) and $E_0 = 65$ kJ mol⁻¹; the second with the lower A factors (TSb) and $E_0 = 54$ kJ mol⁻¹. The curves are positioned to match the data at the pressures of study (as far as is possible). Two features are immediately apparent. First, the fit to experiment is not particularly good for either set of curves. This will be discussed later. Second, the two pairs of curves diverge significantly from one another at the high-pressure limits. Because the high-pressure limiting values of the second-order rate constants, k_1^∞ , for SiH₂ + H₂O are not known, this cannot be used as a criterion to select which fit is best. The following argument, in our view, tends to favor the lower values of k_1^∞ . The temperature dependence of k_1^∞ , regardless of which TS is used, indicates a reduction of value from 296 to 339 K of between 0.80 and 0.70 (10^{-0.10} to 10^{-0.15}) corresponding to E_a of between -4 and -7 kJ mol⁻¹. Thus, the activation energy term, $e^{-E_a/RT}$, of the rate constant at 296 K corresponds to a factor of between 5 and 17. Assuming a value of 10 in combination with each of the assumed A factors leads to values for k_1^∞ of 3×10^{-9} cm³ molecule⁻¹ s⁻¹ for the loose transition state, TSa, and 3×10^{-10} cm³ molecule⁻¹ s⁻¹ for the tight transition state, TSb. The k_1^∞ values found from the modeling lie in the range 1.6–5.0 $\times 10^{-10}$ cm³ molecule⁻¹ s⁻¹. Thus, the tighter TS offers the greatest self-consistency. Because it can be argued that this outcome depends on E_0 , we present in Figure 4 the effect of altering E_0 on these results (for the tighter TSb). The values of E_0 chosen were 48, 54, and 66 kJ mol⁻¹. The comparison is made at 296 K. Clearly, k_1^∞ is lowered by increasing E_0 and raised by lowering E_0 . The looser TSa could be made to produce a lower value for k_1^∞ by increasing E_0 . A value of ca. 77 kJ mol⁻¹ would produce a more self-consistent result, but this is further away from the ab initio value.

Last, because AKL¹⁹ employed a Gorin-type model with certain modes of the loose transition state considered as 2-dimensional internal hindered rotors, we decided to try to introduce the effects of rotation, within the confines of our operational program. This was done first by converting the torsional mode in TSb to an internal rotation. However, because this altered the entropy of activation, small changes in the rocking mode wavenumbers were also made to maintain a constant A factor. Another calculation was done in which the torsions of both the reactant molecule and TSb complex were treated as internal rotations. A third calculation was done in which the vibrational TSb was assumed to include an active overall rotation. The results of these calculations are shown in Figure 5. Clearly any of these offer as good a fit as one another but alter the k_1^∞ value upward (in the case of internal rotations)

or downward (in the case of an external rotation). We do not agree with AKL¹⁹ that treating the low wavenumber torsional vibration as an internal rotation cannot be made to fit our, or indeed their, results provided A and E_0 are appropriately chosen. What these calculations show is that incorporation of such modes will alter the k_1^∞ value. Because this is experimentally unknown (and not measurable under the present conditions), the precise choice of correct model is impossible. Only limits on the combinations of parameters can be set.

Ab Initio Calculations. The potential energy surface for this reaction has been recently studied by HMB²⁰ at the MP2/6-311++G(d,p) and other levels of theory. Our objective, apart from providing an energy surface for interpretation of the experimental results, was to see whether the standard Gaussian compound method (G2 and G3 procedures) would come close to the results of this earlier study. As expected, we found three stable species (or combination of species), viz., (i) H₂Si···OH₂, the initial complex of SiH₂ + H₂O, (ii) SiH₃OH (silanol), the lowest energy species on the surface, and (iii) H₂ + HSiOH (hydroxysilylene in both cis (c) and trans (t) forms). In addition, we have located five transition states, TS1 leading from H₂Si···OH₂ to SiH₃OH, TS2c/TS2t leading from H₂Si···OH₂ to H₂ + HSiOH (c and t) via H₂ elimination, and TS3c/TS3t connecting SiH₃OH to H₂ + HSiOH (c and t). The transition states for H₂ elimination from H₂Si···OH₂ and from SiH₃OH are clearly different from one another.

The structures of all species are shown in Figure 6, and their enthalpy values are listed in Table 3 as well as being represented on the potential energy (enthalpy) surface in Figure 7.

It is worth noting that both TS1 and TS2c/TS2t lie above the threshold energy for reaction, although TS3c/TS3t lie below it.

Discussion

General Comments, Rate Constant Comparisons, and Isotope Effects. The main experimental purpose of this study was to measure the rate constants and their temperature and pressure dependences for the reactions of SiH₂ + H₂O and SiH₂ + D₂O. This has been accomplished and extends the work of AKL¹⁹ who studied SiH₂ + H₂O at 294 K only. Our study was limited to two temperatures by problems of reversibility at higher temperatures. Our results are compared with those of AKL¹⁹ in Table 4. A direct comparison is not possible because the reaction is pressure dependent and we have used a stronger collision partner (SF₆) than AKL,¹⁹ who used Argon. The rate constants differ by a factor of ca. 3 which is reasonable for the difference in efficiencies of the two bath gases. A comparison of the experimental results is shown graphically in Figure 8. The negative temperature dependence of the SiH₂ + H₂O reaction mirrors that of the SiH₂ + CD₃OD reaction also studied by AKL¹⁹ as well as that of many other silylene reactions studied in our labs.^{5–7,9,12,14,15,17}

The isotope effects, k_H/k_D , shown in Table 1 are quite small and, within experimental error, are independent of both temperature and pressure, averaging 1.076 ± 0.080 . There is no sign of any trend. These are typical values for secondary isotope effects and are reminiscent of the values we found previously^{15,18} in the SiH₂/SiD₂ + CH₃CHO reaction. They certainly support a mechanism in which there is no participation of a migrating H (or D) in the rate determining step. These effects are discussed again in the next but one section.

Ab Initio Calculations and the Mechanism. The intermediate species and the transition states together with their structures and energy values are in close agreement with those found by HMB.²⁰ A comparison of energy values is shown in Table 3.

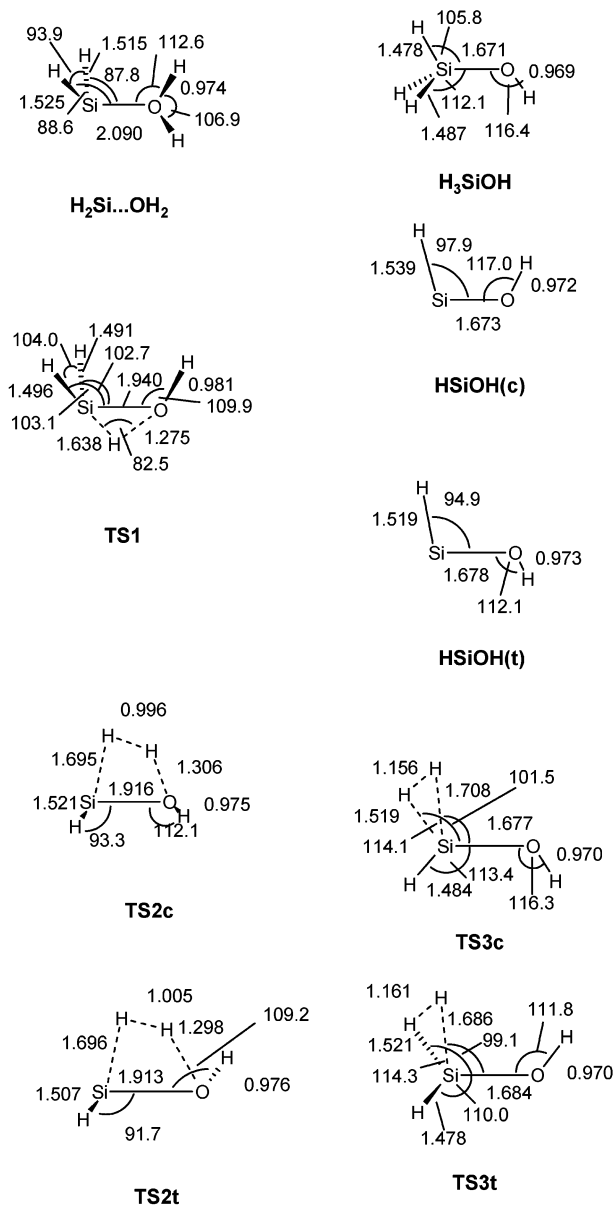


Figure 6. Ab initio MP2=Full/6-31G(d) calculated geometries of local minimum structures and transition states on the $\text{SiH}_2 + \text{H}_2\text{O}$ energy surface. Selected distances are given in Å, and angles are in degrees.

TABLE 3: Ab Initio G3 and G2 Enthalpies for SiH_4O Species of Interest in the $\text{SiH}_2 + \text{H}_2\text{O}$ Reaction

molecular species	G3 enthalpy ^a	relative ^b	G2 enthalpy ^a	relative ^b	HMB ^{b,c}
$\text{SiH}_2 + \text{H}_2\text{O}$	-366.831971	0	-366.492167	0	0
$\text{H}_2\text{Si}\cdots\text{OH}_2$	-366.853159	-56	-366.512523	-53	-53
TS1	-366.822067	+26	-366.480122	+32	+39
H_3SiOH	-366.948156	-305	-366.606833	-301	-294
TS2c	-366.825414	+17	-366.482423	+32	+38
TS2t	-366.825837	+16	-366.482975	+26	+37
$\text{H}_2 + \text{HSiOH(c)}$	-366.880365	-127	-366.538782	-122	-111
$\text{H}_2 + \text{HSiOH(t)}$	-366.880393	-127	-366.538885	-123	-112
TS3c	-366.845726	-36			
TS3t	-366.846611	-38			

^a H_0 (298 K) values in Hartrees. ^b Relative energy in kJ mol^{-1} . ^c Reference 20.

For comparisons with earlier theoretical calculations, the reader is referred to Table 3 of the HMB paper.²⁰ The only points we have added are those of TS3c and TS3t, which were previously found by Zakariah and Tsang.²⁴ What our results show is that

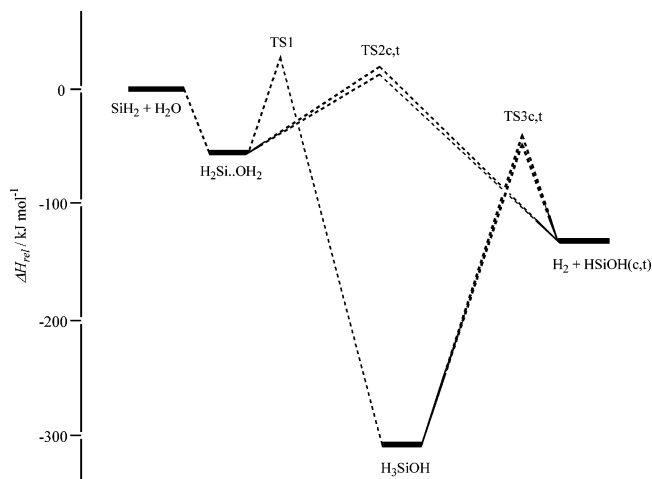


Figure 7. Potential energy (enthalpy) surface for the reaction of $\text{SiH}_2 + \text{H}_2\text{O}$. All enthalpies are calculated at the G3 level.

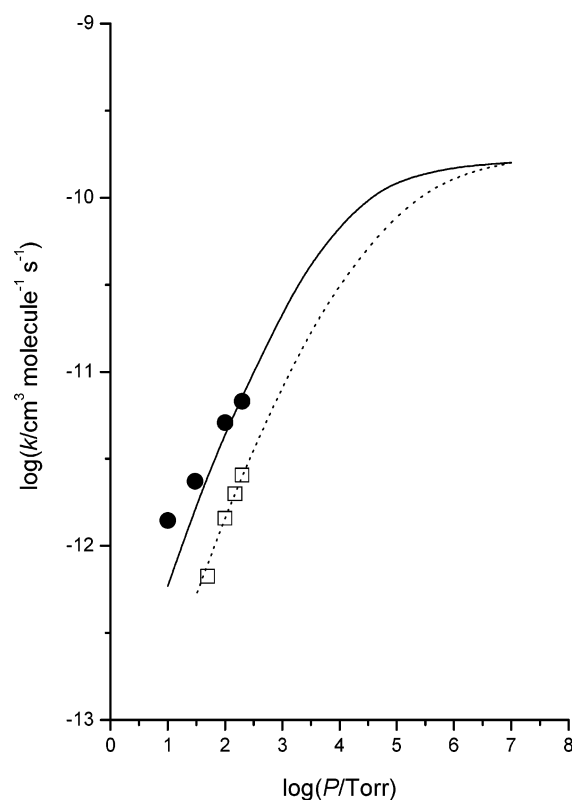


Figure 8. Comparison of pressure dependences of second-order rate constants for $\text{SiH}_2 + \text{H}_2\text{O}$ at 296 K: ●, this work; □, data of ref 19. Lines are RRKM fits based on TSb but with different collisional deactivation step sizes, $\langle\Delta E\rangle_{\text{down}}$: —, 1000 cm^{-1} ; ----, 300 cm^{-1} .

TABLE 4: Comparison of Measured Second-Order Rate Constants^a for $\text{SiH}_2 + \text{H}_2\text{O}$ at Ambient Temperatures

P/Torr	this work ^b	P/Torr	AKL ^c
10	1.40	50	0.67
30	2.35	100	1.44
100	5.10	150	1.99
200	6.76	200	2.55

^a Units of k : $10^{-11} \text{ cm}^3 \text{ molecule}^{-1} \text{ s}^{-1}$. ^b $T = 296 \text{ K}$. ^c Reference 19. $T = 294 \text{ K}$.

there are two potential routes to formation of $\text{H}_2 + \text{HSiOH}$ (c and t) from $\text{H}_2\text{Si}\cdots\text{OH}_2$, one direct and the other via SiH_3OH . However, the important point for the results of the present work is that all pathways from $\text{H}_2\text{Si}\cdots\text{OH}_2$ to products have barriers

in excess of the threshold energy for redissociation to SiH₂ + H₂O, reaction (-1). Thus, our calculations confirm the fact that, after reaction 1 has occurred, there is no easy pathway for the reaction to continue further. The calculations thus support the experimental findings of a pressure dependent association reaction, without involvement of an H-transfer process in the rate determining step. The calculations provide the value for E_0 , the dissociation (or critical) energy for the RRKM modeling studies.

RRKM Modeling Studies. Before discussing the results of the calculations in detail, we show that our RRKM modeling can be made to fit the results of AKL.¹⁹ Using TSb (and $E_0 = 54$ kJ mol⁻¹), we repeated one calculation at 296 K but with $\langle\Delta E\rangle_{\text{down}} = 3.6$ kJ mol⁻¹ (300 cm⁻¹), a reasonable value for Ar bath gas. The result is shown in Figure 8 where it can be seen that good agreement with the experimental data of AKL¹⁹ is obtained. The calculation (from Figure 3) with $\langle\Delta E\rangle_{\text{down}} = 12$ kJ mol⁻¹ (1000 cm⁻¹) is also shown for comparison.

The calculations presented here show that a number of activated complex models can be made to fit (approximately) the experimental data. There are, however, two problems. First, the fit to the data (regardless of model) is not very good. The models all show that in the region of measurement the reaction is approaching its third order region of pressure dependence. The experimental rate constants, particularly at the lower pressures (10 and 30 Torr) do not show such a strong trend with pressure. Increases in k_1 are less than a factor of 2, whereas the pressure change is a factor of 3. It should be acknowledged that, at 10 Torr, the substrate H₂O or D₂O forms a significant proportion of the total gas mixture and differences of collision efficiency between SF₆ and H₂O (or D₂O) may play a role. The measurements of AKL¹⁹ fit their (and our) RRKM calculations better, but the lowest pressure used was 50 Torr and their total pressure range was necessarily limited (50–200 Torr) because of the low collision efficiency of the argon bath gas. The behavior we observe can sometimes arise in complex systems when a non-pressure-dependent competing side reaction becomes significant at low pressures. Although this remains possible, the occurrence of a direct reaction to SiH₃OH or H₂ + HSiOH can be ruled out, not only because the PE surface shows the barriers to be too high but also because such processes involve H-migration and therefore primary isotope effects would become evident at low pressures. Thus, we believe there is some, as yet unexplained, experimental contribution to the rate.³⁵ The second problem concerns the RRKM model. Our modeling shows that the data can be fitted within a range of loose transition states and corresponding critical energies. These models incorporate both internal rotational modes and overall active rotations. None of the fitting is definitive, because we do not have reliable information about the activated complex. This arises in this system because the high-pressure limit which would provide such information does not occur until pressures that are ca. 10⁴–10⁵ times those accessible in our experiments. Because of their preference for a Gorin-type model, AKL¹⁹ found that for their choice of E_0 value (64.9 kJ mol⁻¹) k_1^∞ is 1.3×10^{-9} cm³ molecule⁻¹ s⁻¹ at 294 K. This is in line with their other modeling studies of SiH₂ + CD₃OD¹⁹ and SiH₂ + Me₂O.²¹ The results from these studies have been rationalized with models which produce very high rate constants and positive activation energies at high pressures. The modeling produces a crossover effect in which activation energies switch from negative to positive at a certain pressure. This effect has never been observed by us in any of the SiH₂ systems we have studied, many of which were much closer to the high-pressure limit than

those of the SiH₂ + ROR' systems. AKL¹⁹ have rationalized this modeling outcome by arguing that, in the case of reaction of SiH₂ with O-donor molecules, there may be a long-range interaction giving rise to higher than usual reaction cross sections. Furthermore, they rationalize a positive activation energy by involving a centrifugal potential barrier which is important because of the extended nature of the Si...O bond and the weak binding energy of the zwitterion complex. Although we have no evidence against these propositions, we remain cautious about them, because it seems possible to us that the SiH₂ + ROR' systems can nevertheless be explained within the framework of loose but normal transition states which seem to fit other SiH₂ reaction systems^{5–10,12,15,17,18} and also GeH₂ reaction systems^{36–42} where more weakly bound complexes are generally involved.

It should be added that we have not undertaken variational transition state theory calculations of the isotope effects because of the lack of information about the activated complex. We could have attempted this, as we did for the SiH₂ (SiD₂) + CH₃CHO reaction.¹⁸ However, the exercise undertaken in that work, with a better defined activation complex set of structures, demonstrated that the isotope effects for different degrees of freedom were largely self-canceling, leading to values of k_H/k_D in the range of 1.005–1.122 at the temperatures and pressures of the present work. The calculations in that work combined the high pressure limiting values, 1.097 (296 K) and 1.135 (339 K), with the pressure dependent values (inverse isotope effect) which reduced them by up to 10%. Such an outcome in the present study would be entirely consistent with the experimental results.

Finally, it is interesting to note the conclusion that, in the gas-phase both in this and related systems,^{19,21} the reaction effectively stops at the zwitterion stage; that is, the zwitterion is the actual reaction product! The idea of such species as intermediates in reactions of silylenes with O-donor molecules goes back to the 1980s and the solution studies of Weber's group.^{43–45} Clearly in solution, the zwitterions find ways to react further, and the solvent plays an important role. In the gas phase, the fate of the zwitterions is unclear. We suspect a wall or otherwise catalyzed reaction, which is too slow to affect our measurements.

Acknowledgment. R.B. and R.W. thank Dow Corning for a grant in support of the experimental work. R.B. also thanks the Spanish DGICYT for support under Projects BQU2000-1163-C02-01 and BQU2002-03381.

References and Notes

- (1) Jasinski, J. M.; Becerra, R.; Walsh, R. *Chem. Rev.* **1995**, *95*, 1203.
- (2) Becerra, R.; Walsh, R. Kinetics & mechanisms of silylene reactions: A prototype for gas-phase acid/base chemistry. In *Research in Chemical Kinetics*; Compton, R. G., Hancock, G., Eds.; Elsevier: Amsterdam, 1995; Vol. 3, p 263.
- (3) Gaspar, P. P.; West, R. Silylenes. In *The Chemistry of Organic Silicon Compounds*; Rappoport, Z., Apeloig, Y., Eds.; Wiley: Chichester, U.K., 1998; Vol. 2, Chapter 43, p 2463.
- (4) Becerra, R.; Frey, H. M.; Mason, B. P.; Walsh, R. *Chem. Phys. Lett.* **1991**, *185*, 415.
- (5) Becerra, R.; Walsh, R. *Int. J. Chem. Kinet.* **1994**, *26*, 45.
- (6) Al-Rubaiey, N.; Walsh, R. *J. Phys. Chem.* **1994**, *98*, 5303.
- (7) Becerra, R.; Frey, H. M.; Mason, B. P.; Walsh, R.; Gordon, M. S. *J. Chem. Soc., Faraday Trans.* **1995**, *91*, 2723.
- (8) Becerra, R.; Frey, H. M.; Mason, B. P.; Walsh, R. *J. Organomet. Chem.* **1996**, *521*, 343.
- (9) Al-Rubaiey, N.; Carpenter, I. W.; Walsh, R.; Becerra, R.; Gordon, M. S. *J. Phys. Chem. A* **1998**, *102*, 8564.
- (10) Becerra, R.; Boganov, S. E.; Walsh, R. *J. Chem. Soc., Faraday Trans.* **1998**, *94*, 3569.
- (11) Becerra, R.; Walsh, R. *Int. J. Chem. Kinet.* **1999**, *31*, 393.

- (12) Becerra, R.; Cannady, J. P.; Walsh, R. *J. Phys. Chem. A* **1999**, *103*, 4457.
- (13) Becerra, R.; Carpenter, I. W.; Gutsche, G. J.; King, K. D.; Lawrance, W. D.; Staker, W. S.; Walsh, R. *Chem. Phys. Lett.* **2001**, *333*, 83.
- (14) Becerra, R.; Cannady, J. P.; Walsh, R. *J. Phys. Chem. A* **2001**, *105*, 1897.
- (15) Becerra, R.; Cannady, J. P.; Walsh, R. *Phys. Chem. Chem. Phys.* **2001**, *3*, 2343.
- (16) Becerra, R.; Cannady, J. P.; Walsh, R. *J. Phys. Chem. A* **2002**, *106*, 4922.
- (17) Al-Rubaiey, N.; Becerra, R.; Walsh, R. *Phys. Chem. Chem. Phys.* **2002**, *4*, 5079.
- (18) Becerra, R.; Cannady, J. P.; Walsh, R. *J. Phys. Chem. A* **2002**, *106*, 11558.
- (19) Alexander, U. N.; King, K. D.; Lawrance, W. D. *J. Phys. Chem. A* **2001**, *106*, 973.
- (20) Heaven, M. W.; Metha, G. F.; Buntine, M. A. *J. Phys. Chem. A* **2001**, *105*, 1185.
- (21) Alexander, U. N.; King, K. D.; Lawrance, W. D. *Phys. Chem. Chem. Phys.* **2001**, *3*, 3085.
- (22) Raghavachari, K.; Chandraskhar, J.; Gordon, M. S.; Dykema, K. *J. Am. Chem. Soc.* **1984**, *106*, 5853.
- (23) Su, S.; Gordon, M. S. *Chem. Phys. Lett.* **1993**, *204*, 306.
- (24) Zachariah, M. R.; Tsang, W. *J. Phys. Chem.* **1995**, *99*, 5308.
- (25) (a) Becerra, R.; Cannady, J. P.; Walsh, R. 13th International Symposium on Organosilicon Chemistry, Guanajuato, Mexico, Aug. 26–30, 2002; paper P1–41. (b) Becerra, R.; Cannady, J. P.; Walsh, R. 7th Conference on the Chemistry of Carbenes and Related Intermediates, Kazan, Russia, June 23–26, 2003; paper O17.
- (26) Baggott, J. E.; Frey, H. M.; King, K. D.; Lightfoot, P. D.; Walsh, R.; Watts, I. M. *J. Phys. Chem.* **1988**, *92*, 4025.
- (27) Jasinski, J. M.; Chu, J. O. *J. Chem. Phys.* **1988**, *88*, 1678.
- (28) Frisch, M. J.; Trucks, G. W.; Schlegel, H. B.; Scuseria, G. E.; Robb, M. A.; Cheeseman, J. R.; Zakrzewski, V. G.; Montgomery, J. A., Jr.; Stratmann, R. E.; Burant, J. C.; Dapprich, S.; Millam, J. M.; Daniels, A. D.; Kudin, K. N.; Strain, M. C.; Farkas, O.; Tomasi, J.; Barone, V.; Cossi, M.; Cammi, R.; Mennucci, B.; Pomelli, C.; Adamo, C.; Clifford, S.; Ochterski, J.; Petersson, G. A.; Ayala, P. Y.; Cui, Q.; Morokuma, K.; Malick, D. K.; Rabuck, A. D.; Raghavachari, K.; Foresman, J. B.; Cioslowski, J.; Ortiz, J. V.; Baboul, A. G.; Stefanov, B. B.; Liu, G.; Liashenko, A.; Piskorz, P.; Komaromi, I.; Gomperts, R.; Martin, R. L.; Fox, D. J.; Keith, T.; Al-Laham, M. A.; Peng, C. Y.; Nanayakkara, A.; Gonzalez, C.; Challacombe, M.; Gill, P. M. W.; Johnson, B. G.; Chen, W.; Wong, M. W.; Andres, J. L.; Head-Gordon, M.; Replogle, E. S.; Pople, J. A. *Gaussian 98*, revision A.9; Gaussian, Inc.: Pittsburgh, PA, 1998.
- (29) Curtiss, L. A.; Raghavachari, K.; Redfern, P. C.; Rassolov, V.; Pople, J. A. *J. Chem. Phys.* **1998**, *109*, 7764.
- (30) Gonzales, C.; Schlegel, H. B. *J. Chem. Phys.* **1989**, *90*, 2154.
- (31) Curtiss, L. A.; Raghavachari, K.; Trucks, G. W.; Pople, J. A. *J. Chem. Phys.* **1991**, *94*, 7221.
- (32) Holbrook, K. A.; Pilling, M. J.; Robertson, S. H. *Unimolecular Reactions*, 2nd ed.; Wiley: Chichester, U.K., 1996.
- (33) Chase, M. W., Jr.; Davies, C. A.; Downey, J. R., Jr.; Frurip, D. J.; MacDonald, R. A.; Syverud, A. N. JANAF Thermochemical Tables, 3rd ed.; *J. Phys. Chem. Ref. Data* **1985**, *14*, Supplement 1.
- (34) Hippler, H.; Troe, J. In *Advances in Gas-Phase Photochemistry and Kinetics*; Ashfold, M. N. R., Baggott, J. E., Eds.; Royal Society of Chemistry: London, 1989; Vol. 2, Chapter 5, p 209.
- (35) Further experiments are underway in our laboratories to investigate the low-pressure region in more detail.
- (36) Becerra, R.; Boganov, S. E.; Egorov, M. P.; Nefedov, O. M.; Walsh, R. *Mendeleev Commun.* **1997**, 87.
- (37) Becerra, R.; Boganov, S. E.; Egorov, M. P.; Faustov, V. I.; Nefedov, O. M.; Walsh, R. *J. Am. Chem. Soc.* **1998**, *120*, 12657.
- (38) Becerra, R.; Walsh, R. *Phys. Chem. Chem. Phys.* **1999**, *1*, 5301.
- (39) Becerra, R.; Boganov, S. E.; Egorov, M. P.; Faustov, V. I.; Nefedov, O. M.; Walsh, R. *Phys. Chem. Chem. Phys.* **2001**, *3*, 184.
- (40) Becerra, R.; Walsh, R. *J. Organomet. Chem.* **2001**, *636*, 50.
- (41) Becerra, R.; Boganov, S. E.; Egorov, M. P.; Faustov, V. I.; Promyslov, V. M.; Nefedov, O. M.; Walsh, R. *Phys. Chem. Chem. Phys.* **2002**, *4*, 5079.
- (42) Becerra, R.; Walsh, R. *Phys. Chem. Chem. Phys.* **2002**, *4*, 6001.
- (43) Steele, K. P.; Weber, W. P. *J. Am. Chem. Soc.* **1980**, *102*, 6095.
- (44) Steele, K. P.; Weber, W. P. *Inorg. Chem.* **1981**, *20*, 1302.
- (45) Steele, K. P.; Tzeng, D.; Weber, W. P. *J. Organomet. Chem.* **1982**, *231*, 291.